RESEARCH ARTICLE | MARCH 09 2020

Wavelet entropy-based evaluation of intrinsic predictability of time series

Special Collection: Rare Events in Complex Systems: Understanding and Prediction

Ravi Kumar Guntu ; Pavan Kumar Yeditha ; Maheswaran Rathinasamy ; Matjaž Perc ; Norbert Marwan ; Jürgen Kurths; Ankit Agarwal

Chaos 30, 033117 (2020)
https://doi.org/10.1063/1.5145005

Wavelet entropy-based evaluation of intrinsic predictability of time series

Cite as: Chaos **30**, 033117 (2020); doi: 10.1063/1.5145005
Submitted: 13 January 2020 · Accepted: 17 February 2020 ·
Published Online: 9 March 2020

Ravi Kumar Guntu,[1] Pavan Kumar Yeditha,[2] Maheswaran Rathinasamy,[2] Matjaž Perc,[3,4,5] Norbert Marwan,[6] Jürgen Kurths,[6,7] and Ankit Agarwal[1,a)]

AFFILIATIONS

[1]Department of Hydrology, Indian Institute of Technology Roorkee, Roorkee 247667, India
[2]Department of Civil Engineering, MVGR College of Engineering, Vizianagaram 535005, India
[3]Faculty of Natural Sciences and Mathematics, University of Maribor, 2000 Maribor, Slovenia
[4]Center for Applied Mathematics and Theoretical Physics, University of Maribor, 2000 Maribor, Slovenia
[5]Department of Medical Research, China Medical University Hospital, China Medical University, Taichung 40402, Taiwan
[6]Potsdam Institute for Climate Impact Research, Telegrafenberg, 14412 Potsdam, Germany
[7]Institute of Physics, Humboldt University, 12489 Berlin, Germany

Note: This article is part of the Focus Issue, Rare Events in Complex Systems: Understanding and Prediciton.
[a)]**Author to whom correspondence should be addressed:** agarwal.10891.ankit@gmail.com

ABSTRACT

Intrinsic predictability is imperative to quantify inherent information contained in a time series and assists in evaluating the performance of different forecasting methods to get the best possible prediction. Model forecasting performance is the measure of the probability of success. Nevertheless, model performance or the model does not provide understanding for improvement in prediction. Intuitively, intrinsic predictability delivers the highest level of predictability for a time series and informative in unfolding whether the system is unpredictable or the chosen model is a poor choice. We introduce a novel measure, the Wavelet Entropy Energy Measure (WEEM), based on wavelet transformation and information entropy for quantification of intrinsic predictability of time series. To investigate the efficiency and reliability of the proposed measure, model forecast performance was evaluated via a wavelet networks approach. The proposed measure uses the wavelet energy distribution of a time series at different scales and compares it with the wavelet energy distribution of white noise to quantify a time series as deterministic or random. We test the WEEM using a wide variety of time series ranging from deterministic, non-stationary, and ones contaminated with white noise with different noise-signal ratios. Furthermore, a relationship is developed between the WEEM and Nash–Sutcliffe Efficiency, one of the widely known measures of forecast performance. The reliability of WEEM is demonstrated by exploring the relationship to logistic map and real-world data.

This study explores the application of wavelet energy function and entropy for possible quantification of intrinsic predictability of a time series in terms of the Wavelet Energy Entropy Measure. One of the advantages of the proposed measure is that it considers the dynamics of the process spread across different time scales, which other similarity measures of predictability have not considered explicitly. Furthermore, the proposed measure is linked to forecasting performances. The proposed measure can be used for estimating the intrinsic predictability of a time series, understanding the capability of models in capturing the underlying system, and among others.

I. INTRODUCTION

Time series predictability is a measure of how well future values of a time series can be forecasted,[1] where a time series is a sequence of observations $\{X_t, t = 1, 2, 3, \ldots, N\}$. A time series generated by a deterministic process has high predictability, and its future values can be forecasted very well from its past values. However, the one by an uncorrelated stochastic process has low predictability, and its past values provide only a statistical characterization of the future values.[2] According to Pennekamp *et al.*, predictability can be classified into realized (achieved predictability of a system from a given forecasting model) and intrinsic (maximum achievable predictability of a system[4]) predictability.[3] The former indicates the

forecast performance of models and is generally quantified as the correlation coefficient among predicted and observed values or its complement error measures such as Nash–Sutcliffe Efficiency. Different models will provide different levels of realized predictability and just from the realized predictability, it is impossible to say whether the system is complex or the model is a poor choice. By contrast, the intrinsic predictability of a time series (or the underlying system) is an absolute measure that represents the highest achievable predictability.[1,4] For instance, a time series having a complete predictive structure has high intrinsic predictability. Periodic and constant signals fall in this category. On the contrary, a fully complex signal (e.g., white noise) that is generated by an uncorrelated process has no intrinsic predictability and attains low forecasting performance for deterministic chaotic processes with low correlation (e.g., logistic map for certain parameters).

Generally, the intrinsic predictability can be measured using model-free measures of time series complexity. Some of these measures include Lyapunov exponents,[5] recurrence measures,[6–8] network measures,[64] and information entropic measures.[9,10] Comparatively, entropic measures have received more popularity owing to its simplicity in calculating the intrinsic predictability, in particular within the fields of human mobility,[11] stock price returns,[12] patient health records,[13,14] and also in nonlinear climatic systems.[15–19] The range of entropy varies from highest for a white noise process and to lowest in case of the deterministic chaotic processes (e.g., logistic map for certain parameters).[20,21]

Indeed, entropy measures have contributed significantly to our existing knowledge on time series predictability. Still, there is a substantial scope of advancement, in particular, while considering the underlying system whose dynamics are spread over different time scales. In such systems, it is entirely plausible that deterministic features present at a specific scale might be concealed while examining the process at a different time scale. Doss-Gollin *et al.* stressed the necessity of considering the multiscale dynamics across different time scales for robust adaptation.[21] Maheswaran and Khosa emphasized the need for multiple-scale analysis for effective forecasting of hydrological processes.[22] According to Barrat *et al.*, specific climate-related processes are highly complex due to the scale-emergent occurrences owing to the nonlinear dynamic process and long-memory temporal connections.[23] These studies and several others[24–28] indicate the presence of features of multiple time scale phenomena, and these often get camouflaged in the observed time series. Li and Zhang showed that the traditional measures based on entropy fail to estimate the predictability at multiple time scales.[29]

In recent decades, the Wavelet transform is competent in comprehending multiscale dynamical processes across time scales.[25,30] With the capability to enable multi-scale resolution and frequency localization in time, wavelets offer the advantage of facilitating the decomposition of the given time series into its various, but scale-specific, dynamic components as proxies of the corresponding physical processes at those scales.[31] Numerous wavelet applications in terms of wavelet energy via global power spectrum have been reported in the recent past and widespread in the fields of hydrologic regionalization,[32] climate downscaling,[33] dynamical systems,[62,63] and complexity of time series.[19,20,34–36]

In this study, we combine wavelet and information entropy to propose a novel measure called Wavelet Entropy Energy measure (WEEM). The proposed measure is validated using a set of constructed signals ranging from white noise to deterministic processes. Furthermore, we connect WEEM to well-known forecast measure (Nash–Sutcliffe Criteria) using a state-of-the-art forecasting model based on Wavelet Neural Networks. This link between intrinsic predictability and realized predictability helps in comparing the intrinsic predictability of different systems and provides a guideline on model selection. To test the strength of the relationship, we apply it to logistic map time series and 4500 real-world rainfall time series of the Indian subcontinent. We select monsoon rainfall since it is one of the most critical climate element affecting the livelihood and wellbeing of the society. The variability, strength, onset, and withdrawal of monsoonal rainfall have an enormous effect on Indian agriculture, economy, life, and prosperity of the inhabitants of the Indian subcontinent. Consequently, understanding the mechanisms of the Indian monsoon and its successful forecasting is not only a question of great scientific interest but also a significant societal challenge.

The remainder of the paper is organized as follows: Section II describes the development of the proposed measure, and Sec. III introduces the selected model signals and real-time series. The results are discussed in Sec. IV. Our conclusions are summarized in Sec. V.

II. METHODS

Here, we describe the methodology for the proposed WEEM. Here, we combine two already well-established approaches, *information entropy* and *continuous wavelet transform* (CWT), to quantify the time series predictability. The following sub-sections briefly introduce Information entropy and wavelets and subsequently provide the mathematical framework for WEEM.

A. Information entropy

The Information entropy originally proposed by Shannon[37] is described as

$$IE(X) = -\sum_{i=1}^{N} P(x_i)\log_2[P(x_i)], \quad (1)$$

where $X = \{x_1, x_2, x_3, x_4, \ldots X_N\}$ is the sample space with all possible states; $P(x_i)$ is the probability of occurrence of the random event x_i; $0 \le P(x_i) \le 1$; $\sum_{i=1}^{N} P(x_i) = 1$; $-\log_2 P(x_i)$ is the information of uncertainty about the event x_i occurring with $P(x_i)$; IE(X) is the entropy of X in bits; and N is the number of states. Entropy is an outcome of the process of a random variable, which can address the uncertainty of the system by giving information about the random variable.[38,39] The entropy concept is equally valid for deterministic and stochastic processes.[20,40] In general, higher entropy indicates random systems. Therefore, white noise processes which are almost unpredictable have the highest entropy.[20,29]

B. Wavelet transform

The wavelet transform is an expedient method for converting a time series into a new form, which consists of inherent features of the original time series.[41] It is defined as the convolution of

the signal with scaled, shifted versions of the wavelet function ψ.[42] Generally, the wavelet transform can be classified into Continuous Wavelet Transform (CWT) and Discrete Wavelet Transform. In this study, we use CWT to quantify the intrinsic predictability. The mathematical representation of CWT is as follows:

$$WT(\alpha, q) = \frac{1}{\sqrt{\alpha}} \int_{-\infty}^{\infty} x(t) \hat{\psi} \left(\frac{t - q}{\alpha} \right) dt \qquad \text{with}$$
$$\psi(t) = \frac{1}{\pi^{\frac{1}{4}}} \left(e^{i2\pi f_o . t} \right) e^{\frac{-t^2}{2}}, \tag{2}$$

where f_o is the central frequency of the morlet wavelet; α and q are scale and translation parameters; and $\hat{\psi}(t)$ is the complex conjugate of the wavelet function $\psi(t)$.

The wavelet transform as defined by Eq. (2) is a CWT because the scale and time parameters, α and q, assume continuous values. It provides a redundant representation of a signal as the CWT of a function at scale "α" and location "q" can be obtained from the CWT of the same function at other scales and locations. Since the CWT acts as an orthonormal basis decomposition, it can be shown that it is also isometric as it preserves the overall energy content of the signal and, thereby, allowing recovery of the function x(t) from its transform by using the following reconstruction formula:[41]

$$x(t) = \frac{1}{C_w} \int_0^{\infty} \left[\int_{-\infty}^{\infty} |WT(\alpha, q)|^2 \psi_{(\alpha,q)}(t) dq \right] \frac{d\alpha}{\alpha^2}, \tag{3}$$

where c_w is a constant depending on the type of the mother wavelet. The scale-wise energy $E(\alpha)$ of the signal x(t) can be represented under level α as

$$E(\alpha) = \int_{-\infty}^{\infty} [x(t)]^2 dt = \frac{1}{C_w} \int_0^{\infty} \left[\int_{-\infty}^{\infty} |W(\alpha, q)|^2 dq \right] \frac{d\alpha}{\alpha^2}. \tag{4}$$

The left-hand side of the above equation is the energy of the signal x(t).[41] We can, thus, interpret $|W(\alpha, q)|^2 dq$ as being proportional to an energy density function that decomposes the energy in x(t) across different scales and times. If $|W(\alpha, q)|^2 dq$ is large (small), we can say that there is an important (insignificant) contribution to the energy in x(t) at scale α and time q. For a white noise process, the energy distribution is uniform across scales, and the entropy of the energy distribution will be maximum. On the other hand, for a deterministic distribution, the entire energy gets concentrated to one scale, and we obtain minimum entropy.

C. Wavelet energy entropy measure (WEEM)

To measure the energy distribution of a time series, using Morlet[60,61] as the mother wavelet, the wavelet coefficients $W(\alpha, q)$ can be obtained from Eq. (2). Once the wavelet coefficients are obtained, the wavelet energy ($E(t, \alpha)$) under time position t and scale α is computed as per Eq. (4) across each scale. The total wavelet energy upto scale n is calculated as $TE = \sum_{\alpha=1}^{n} E(\alpha)$. From the wavelet energy distribution across all the scales $\alpha = 1, 2, 3, \ldots, n$, the probability density function is calculated as $P(\alpha) = \frac{E(\alpha)}{\sum_{\alpha=1}^{n} E(\alpha)}$. From the likelihood of each level, the continuous wavelet entropy for the time series is calculated as

$$CWE = -\frac{E(\alpha)}{\sum_{\alpha=1}^{n} E(\alpha)} \log_2 \frac{E(\alpha)}{\sum_{\alpha=1}^{n} E(\alpha)}. \tag{5}$$

For quantification of the intrinsic predictability, we consider a reference process having maximum entropy with no predictive information. Hence, the white noise process is viewed as a reference process due to its scattered energy distribution across all scales. It is highly unpredictable compared to any other processes in space and time and has the highest entropy.[20] In the present study, as per Sang *et al.*, we generate white noise time series with the same length of original time series having mean of original time series and standard deviation of unity.[20] Continuous wavelet entropy for white noise time series can be calculated using Eq. (5).

Finally, the Wavelet Energy Entropy Measure (WEEM) is proposed as

$$WEEM = \frac{2^{CWE_R} - 2^{CWE_O}}{2^{CWE_R}}, \tag{6}$$

where CWE_O and CWE_R are the continous wavelet entropy of the original time series and white noise series, respectively. The value of WEEM ranges from 0 to 1. If WEEM is nearer to one, then the time series has high intrinsic predictability, and this is due to the entire energy gets concentrated to few scales. In contrary, if WEEM is near to zero, the time series has a scattered distribution of wavelet energy almost similar to that of a white noise process and has a very low intrinsic predictability. The schematic of the calculation of the WEEM is shown in Fig. 1.

D. Forecasting with Wavelet Neural Networks

For estimating the forecasting error or the realized predictability, we use a state-of-the-art forecasting model Wavelet Neural Networks (WNNs), which has been tested for its reliability in several studies. WNN is a coupled model combining wavelet analysis and artificial neural networks. WNNs have outperformed stand-alone models like artificial neural networks, multiple linear regression, and autoregressive approach and proved to be robust in forecasting various fields of geophysical variables.[43,44] The neural network uses the detailed components of time series as inputs and picks up the underlying variability in the time series at different scales;[32,33] minute details are well captured.[44] For the wavelet analysis, we have chosen a prominent and straightforward db4 wavelet, and the time series is decomposed up to ten levels following the procedure outlined in Ref. 31. For more details on wavelet analysis and selection of suitable mother wavelet, the readers are referred to Ref. 31. For the simulation of neural networks, we have used the Levenberg–Marquardt algorithm to train the Neural Network model because it is fast, accurate, and reliable.[44,45] In addition, several studies show that the algorithm is robust in terms of statistical significance and processing flexibility.[46,47] The model is initially trained for 70 percentage of the data by providing both input and target to the model. In this procedure, the model understands the relationship between the predictor and predictand. The model is trained until the results are convergent within the desirable limits of high accuracy and less error components. Then in case of validation, only the inputs, i.e., the remaining 30 percent of data, are provided to the created network and tested

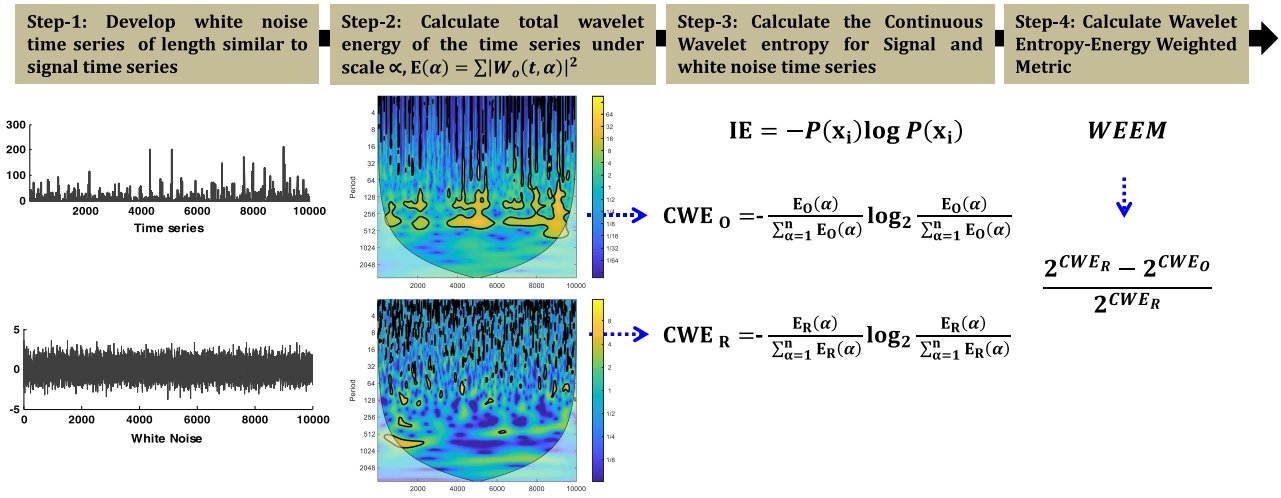

FIG. 1. Development of the WEEM. Step-1 generation of a white noise time series similar to the data length of the original signal with zero mean and unit standard deviation. Step-2 obtains wavelet power spectrum for the original signal as well as for the white noise time series. The y axis in the figure represents the wavelet scale, and the x axis is time (unit). Compute the global wavelet spectrum from the wavelet spectrum at each scale. Calculate the total energy at every scale p. Step-3 calculation of continuous wavelet entropy from the global wavelet spectrum for the original signal (CWE_O) as well as for the white noise time series (CWE_R). Step-4 from the obtained CWE_O and CWE_R compute the proposed measure WEEM.

to simulate the respective predictand with same amounts of accuracies as of training stage. The optimal number of hidden neurons for each of the model was found using the trial and error procedure. The number of hidden neurons was varied from 10 to 20, and the best value was chosen based on the RMSE.[48] See text S2 in the supplementary material for further detailed description of WNNs.

1. Assessment of forecasting performance

In the present study, we first quantify the forecasting performance of WNNs using Nash–Sutcliffe Efficiency (NSE),[49]

$$\mathrm{NSE} = 1 - \left[\frac{\sum_{j=1}^{p} (X_j^{obs} - X_j^{sim})^2}{\sum_{j=1}^{p} (X_j^{obs} - X_j^{mean})^2} \right], \tag{7}$$

where X_j^{obs} is the jth observation of the original time series being estimated, X_j^{sim} is the jth simulated value for the original time series being estimated, X_j^{mean} is the mean of the original time series for the constituent being evaluated, and p is the number of observations. The range of NSE varies from $-\infty$, i.e., high forecasting error, to 1, i.e., zero forecasting error.

III. DATA AND STUDY DESIGN TO TEST WEEM

The datasets used in this study consist of constructed signals with predefined properties and real-world data. In the first part, we attempt to develop a relationship between NSE and WEEM using model signals. Furthermore, this relationship is tested using the logistic map and real-world data. These tests aim to understand the performance of WEEM in quantifying the intrinsic predictability of linear and non-linear processes.

A. Constructed signals with predefined properties data for the establishment of the relationship between WEEM and NSE

For developing a relationship between the intrinsic predictability and forecast performance, following the approach of Agarwal *et al.* and DelSole, we generate several varieties of constructed signals ranging from deterministic, non-stationary to stochastic.[30,50] The details of the case studies and the wavelet power spectra are given in Table I and Fig. 2, respectively. See text S1 in the supplementary material for the procedure of constructed signals.

B. Case I: Deterministic time series

A single constructed signal is generated following the approach of Agarwal *et al.* to know the behavior of WEEM for a complete deterministic time series without the presence of noise.[30] Figure 2 (panel I) shows the CWT of the signal, and it can be seen that the energy is getting concentrated in a few number of scales.

C. Case II: Non-stationary time series

Following the approach of Agarwal *et al.*, a non-stationary time series encompassing five sine waves with different frequencies (z1–z5) is considered.[30] This time series possess features that are frequently found in climate and geophysical data, where high frequency, small-scale processes are superimposed on low-frequency, coarse-scale processes.[51] Figure 2 (panel II) show the CWT of this time series, and it can be seen that the energy is scattered to more number of scales.

TABLE I. Details of constructed signals with predefined properties. The data are in three categories, i.e., signals with physical characteristics of (I) stationary signal, (II) non-stationary signal, and (III) stationary signal contaminated with white noise.

Case	Mathematical expression	Other details	Reference
I	Sinusoidal stationary signal $S1 = S$	$S = \sin(2\pi t/16)$, where $t = 1, 2, 3, \ldots, 40\,000$	Agarwal *et al.*[30]
II	Non-stationary signal $S1 = z1 + z2 + z3 + z4 + z5$	$z1 = \sin\left(500\pi\left(\frac{t}{16}\right)^{0.5}\right)$ $z2 = \sin\left(250\pi\left(\frac{t}{16}\right)^{0.5}\right)$ $z3 = \sin\left(125\pi\left(\frac{t}{16}\right)^{0.5}\right)$ $z4 = \sin\left(62.5\pi\left(\frac{t}{16}\right)^{0.5}\right)$ $z5 = \sin\left(31.25\pi\left(\frac{t}{16}\right)^{0.5}\right)$ where $t = 0, 0.01, 0.02, \ldots, 400$	Agarwal *et al.*,[30] Yan and Gao,[52] and Hu and Si[51]
III	Sinusoidal stationary signal contaminated with white noise $S1 = S + \frac{\text{noise}}{\text{signal}} \sim 0.1$ $S2 = S + \frac{\text{noise}}{\text{signal}} \sim 0.2$ $S3 = S + \frac{\text{noise}}{\text{signal}} \sim 0.3$ $\ldots$ $S200 = S + \frac{\text{noise}}{\text{signal}} \sim 20$	$S = \sin(2\pi t/16)$, $\frac{\text{noise}}{\text{signal}} \sim n$ where $n = 0.1, 0.2, \ldots, 20$	DelSole[50]

D. Case III: Stochastic time series

Here, 200 sinusoidal stationary signals contaminated with white noise are generated (see Table I) following the approach of DelSole.[50] Original time series is contaminated with the white noise of varying noise-signal (N/S) ratios ranging from 0.1 to 20. The purpose of Case III is to investigate the ability of the measure in assessing the uncertainty of energy distribution across scales for a contaminated time series with varying N/S ratios.

1. Testing WEEM with logistic map

Next, we investigate the proposed measure to the well-known population model, the logistic map,

$$x_{n+1} = r x_n (1 - x_n). \tag{8}$$

This model maps the future population size (x_{n+1}) as a function of the past time step population size (X_n) in a discrete approach showing a nonlinear phenomenon for growth rate $r \in (1, 4)$. This time series exhibits a wide range of dynamical behavior from fixed point and oscillatory motion to chaotic behavior.[3] A complete description of the logistic map and its nonlinear transformation can be found in Trulla *et al.*[53] From the wide variety of nonlinear phenomena, we selected the logistic map, especially in the interesting range of growth rate $r \in (3, 4)$ with a step width of $\Delta r = 0.0015$. We are, in particular, interested in the capability of the intrinsic predictability for laminar states in chaos–chaos transitions. Therefore, for each r, we generate time series of the length with 2000 time steps. The last 1000 time steps are only considered and first 1000 transients are ignored for further analysis.

2. Testing WEEM with real-world data

We also applied the proposed measure to real-world data. For this purpose, we considered 4500 daily rainfall time series, which are extracted from the $0.25° \times 0.25°$ gridded dataset developed by Pai *et al.*,[54] spread all over the Indian mainland. We have used 113 years of daily rainfall from 1st January 1901 to 31st December 2013, which is available at the National Climate Center of India Meteorological Department. Data processing and quality control were performed according to Rajeevan *et al.*[55]

IV. RESULTS

To quantify the intrinsic predictability, which can be expressed in terms of the entropy of energy distribution of a time series, we decompose the given time series up to n scales using the Morlet wavelet. There are several other mother wavelets that could be used for wavelet decomposition; however, it has been demonstrated that the choice of the mother wavelets does not affect the results to a great extent.[25]

For the case I, the measure is tested for the stationary sinusoidal time series for 1000 times and the 95th percentile value of WEEM is very close to 0.93 indicating that the spread of the energy distribution is confined to few scales, thereby less uncertainty and intrinsic predictability is very high.

For case II, the wavelet power spectrum is plotted (see Fig. 2, Panel II), and it describes the non-stationary phenomenon, time-dependent features at higher scales $2 \leq \lambda \leq 6$. In this particular case, WEEM ≈ 0.688. The spread of energy distribution

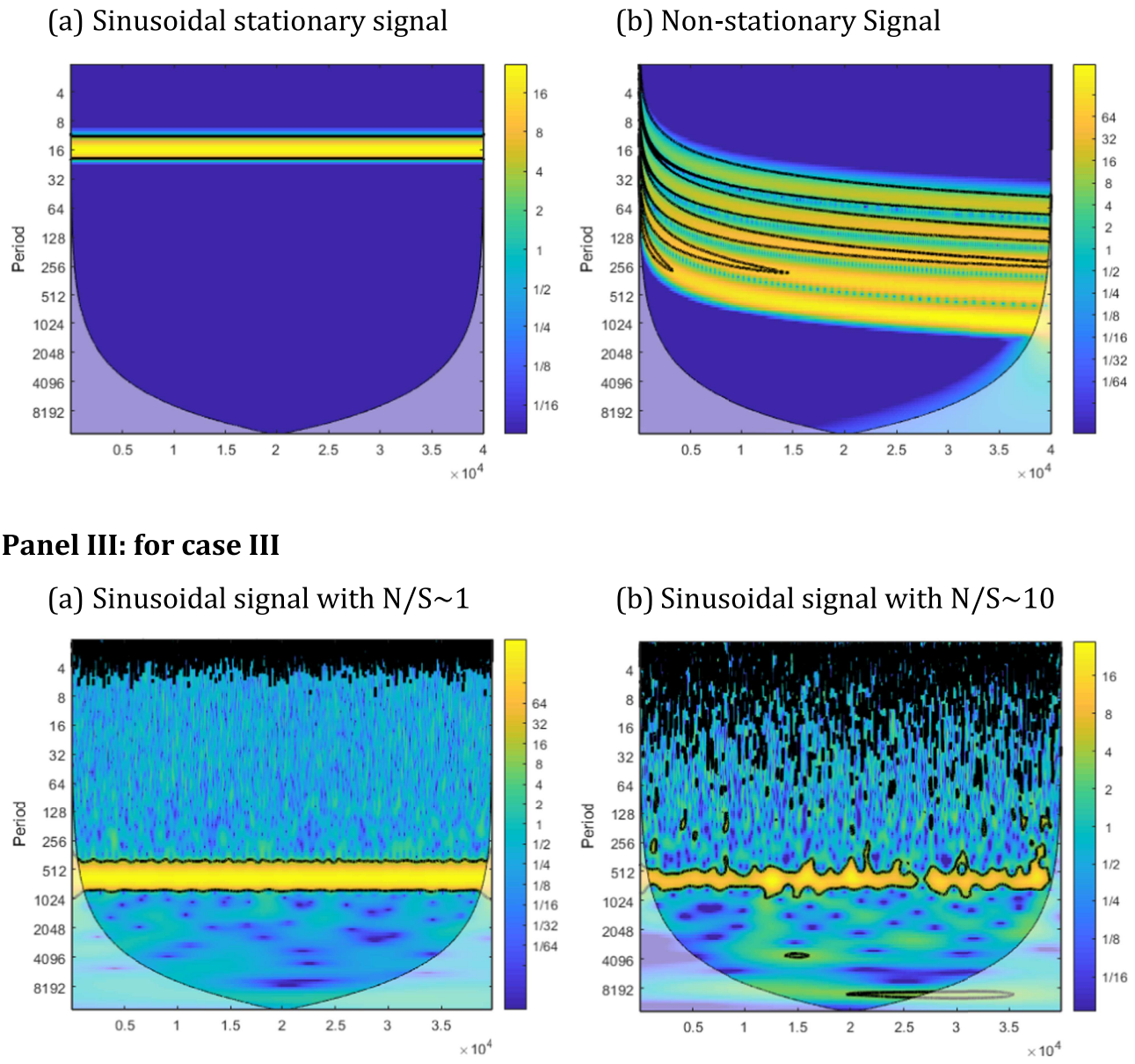

FIG. 2. Wavelet power spectra of constructed signals (Table I). Panel I: sinusoidal stationary signal (S1) for case I; Panel II: non-stationary signal (S1) for case II. Panel III: sinusoidal stationary signal contaminated with white noise of (a) N/S ∼ 1 (S10) and (b) N/S ∼ 10 (S100), respectively, for case-III; in all the panels, the y axis represents the corresponding Fourier period = 2^p, where p = wavelet scale and the x axis represents the time. The thick contour encircles spots of greater than 95% confidence for a red-noise process (increasing power with decreasing frequency).

is not confined to a few scales. WEEM indicates that the uncertainty of the energy distribution is larger than the case I, and there is less scope for intrinsic predictability for non-stationary signals.

For case III, the wavelet power spectrum for the deterministic signal contaminated with white noise for two N/S ratios is shown in Fig. 2, panel III. To construct a confidence interval for WEEM, we generate 1000 white noise time series having zero mean and

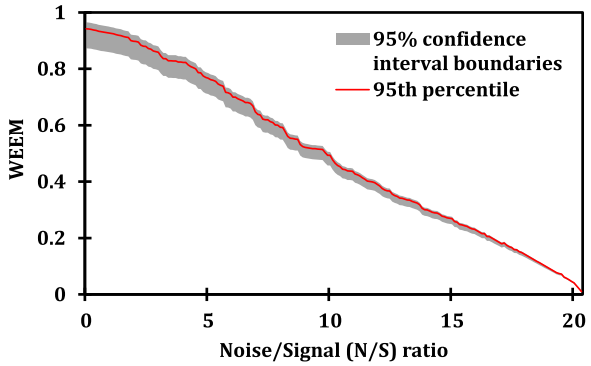

FIG. 3. WEEM as a function of the noise/signal ratio. The abscissa represents the N/S ratio of 200 stationary contaminated with white noise scaled from 0.1 to 20. The range and average of WEEM for each N/S ratio are represented on the ordinate.

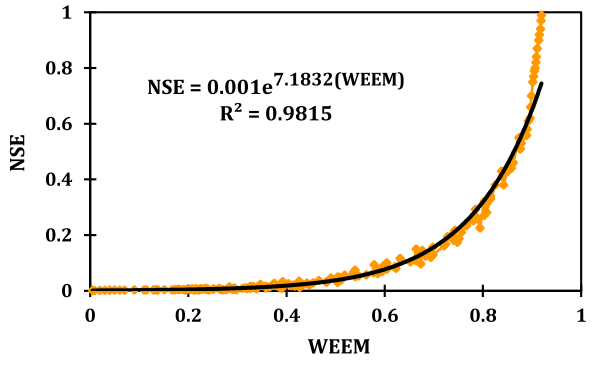

FIG. 5. Scatterplot between WEEM and NSE based on the obtained values of WEEM, NSE from the forecasting model for 200 constructed signals as described for case III in Fig. 2. The black line is the best fitted exponential equation for the relationship between WEEM and NSE, where 98 percentile of the variance of NSE can be explained using WEEM.

standard deviation of unity. Then, each of the 1000 time series is used as CWE_R in Eq. (6) to calculate the WEEMs for the given original time series. The 95th percentile of these obtained 1000 WEEMs is reported as the intrinsic predictability of time series, and 2.5th and 97.5th percentiles are used as the 95% confidence interval boundaries (see Fig. 3). As the ratio increases, the WEEM value decreases with N/S and becomes zero for a ratio of 20. It indicates that the spread of the energy distribution across various scales is similar to a white noise process and the influence of noise is strong over the deterministic component resulting in a substantial loss of information. In contrary, if the ratio lies between 1 and 2, then the spread of energy distribution is limited to few scales in addition to that the influence of noise on energy concentration is also negligible. Therefore, the intrinsic predictability of a time series will be very high due to high deterministic feature conjunction with insignificant noise. Figure 4 shows a trend of CWE_O with 95th percentile WEEMs, and it reveals that intrinsic predictability increases with a decrease in CWE_O.

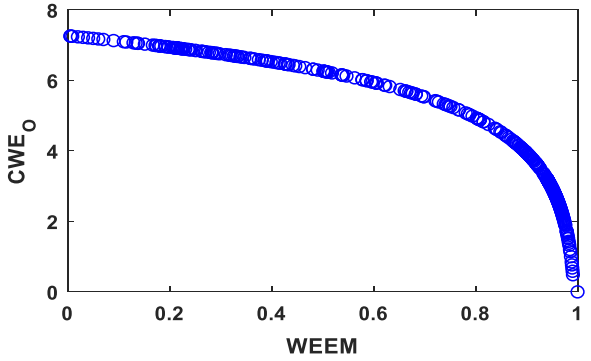

FIG. 4. Scatterplot between 95th percentile of WEEM and its corresponding CWE_O. As the CWE_O decreases, intrinsic predictability increases, and it becomes one when CWE_O is zero.

A. Relationship between intrinsic predictability and forecasting performance

Even though WEEM enables quantification of the intrinsic predictability, for practical application, it needs to be linked to the forecasting performance or realized predictability.[3] For this purpose, the above 200 constructed signals were simulated using the robust WNN's model (see Appendix S1 in the supplementary material), and the forecast performance was estimated for each of the time series. Figure 5 shows the scatterplot between the WEEM and NSE values and the corresponding regression relationship. There exists an exponential relationship between the forecasting performance and the WEEM.

The best-fit equation

$$\mathrm{NSE} = 0.001e^{7.1832(\mathrm{WEEM})} \tag{9}$$

with the coefficient of determination (R^2) ≈ 0.98 was found to capture the relationship between forecasting performance and WEEM. With the above linkage, the interpretation of WEEM becomes more apparent and more comparable.

B. Reliability assessment of WEEM with logistic map

To demonstrate the reliability of (i) WEEM in handling nonlinear complex systems and (ii) the relationship between WEEM and NSE, we have used the logistic map. Figure 6(a) shows the nonlinear phenomenon of population change from a predictable mode to a chaotic one. The obtained WEEM for different r values is plotted in Fig. 6(b). At $r = 3.1$, the system is in a periodic regime, and future values will be taking only two values and as r increases a bifurcation takes from original two values into four and so on until r reaches 3.6. Between $r = 3.1$ and 3.56995, the system is completely predictable and the WEEM values are almost 1, disclosing that the system in that window has high intrinsic predictability. As the growth rate increases to 3.7, nonlinear phenomena unveil a rapid transition from complete deterministic to chaotic behavior, and at $r = 4$, the time series has the highest level of complexity with almost no intrinsic

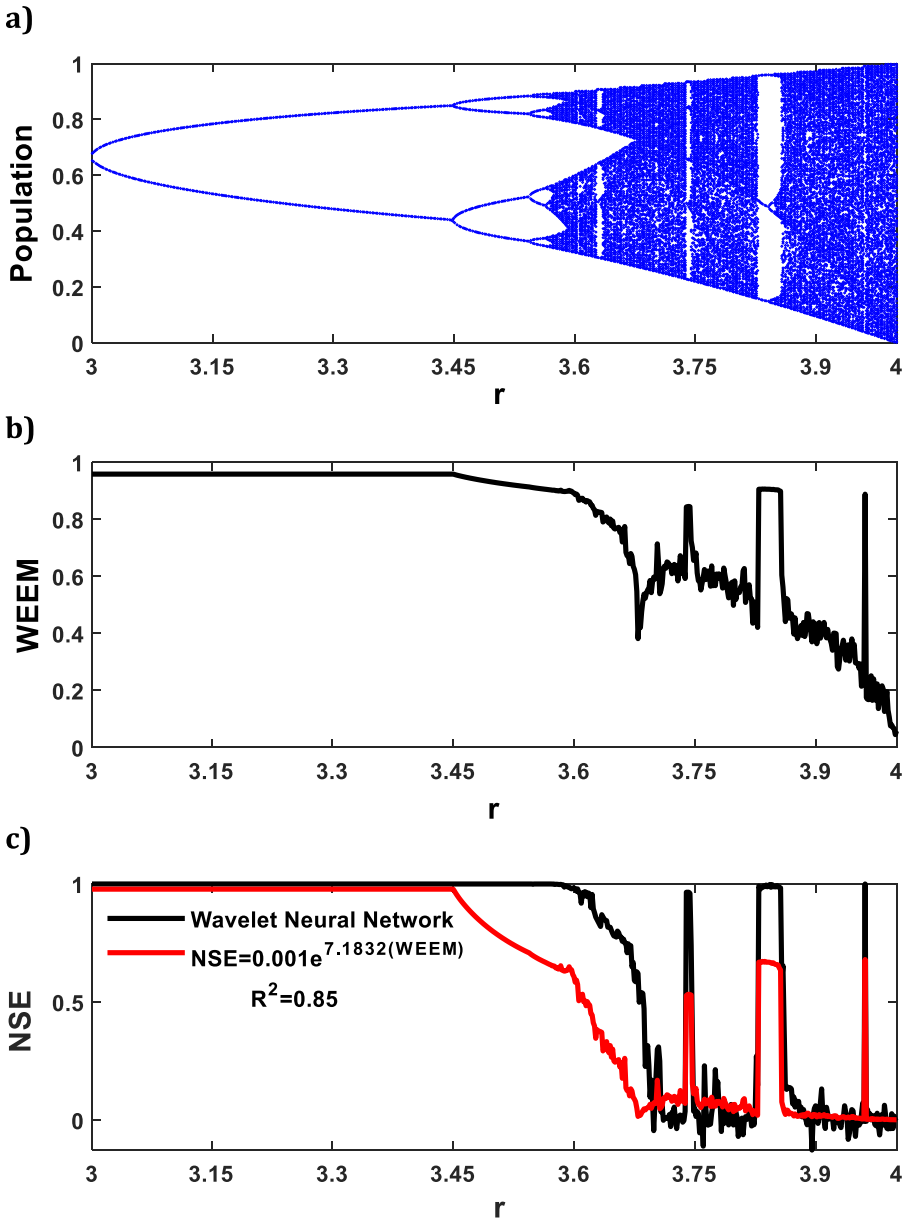

FIG. 6. Overview of the reliability of the WEEM. (a) We applied WEEM to time series from a well-known population dynamic model, the logistic map, and the image shows the nonlinear phenomenon of population change on ordinate for a growth rate (r) between 3 and 4 on the abscissa. When r is in between 3 and 3.56995, the system will be in the periodic regime and will be completely predictable. As r reaches 3.56995, the system changes to chaotic dynamics, and it becomes less and less predictable until r reaches 4. (b) WEEM against r values. The abscissa represents r values from 3 to 4, and the obtained WEEM value is presented on the ordinate. When r is in between 3 and 3.56995, the WEEM is close to 1, the system is predictable and interpretation is convergent with the logistic map. (c) Validation of the proposed relationship between NSE and WEEM for different r values and the possible NSE values were estimated using the relationship, and the actual NSE values obtained from model prediction are presented in red and black lines.

predictability. For r = 3.7 to 4, the WEEM value gradually decreases, indicating that the possibility of getting future values based on the past data is extremely low and has a very low intrinsic predictability due to chaotic behavior. NSE values are estimated using the relationship $NSE = 0.001e^{7.1832(WEEM)}$, and the real forecasting performance NSE was obtained from the simulation of WNNs. Figure 6(c) represents the estimated and obtained NSE values with red and black lines, respectively. The plot shows that the proposed linkage between NSE and WEEM is robust and reliable and is comparable with NSE obtained from the WNN model. As a corollary, this also shows the strength of WEEM in capturing the intrinsic predictability of periodic windows also partially visible.

C. Application and assessment of WEEM with real-world data

After testing the efficiency of WEEM in quantifying the intrinsic predictability for some prototypical situations, we apply the WEEM to real-world time series, i.e., observed daily rainfall in the Indian subcontinent. The 95th percentile of WEEM values for all the stations is obtained, and the spatial distribution of WEEM for the Indian country is plotted in Fig. 7(a). The minimum value of WEEM is 0.16, and the highest value is approximately equal to 0.78, delineating the Indian country into six zones. The regions with blue color revealing a spread of dominant energy are concentrated only to a few

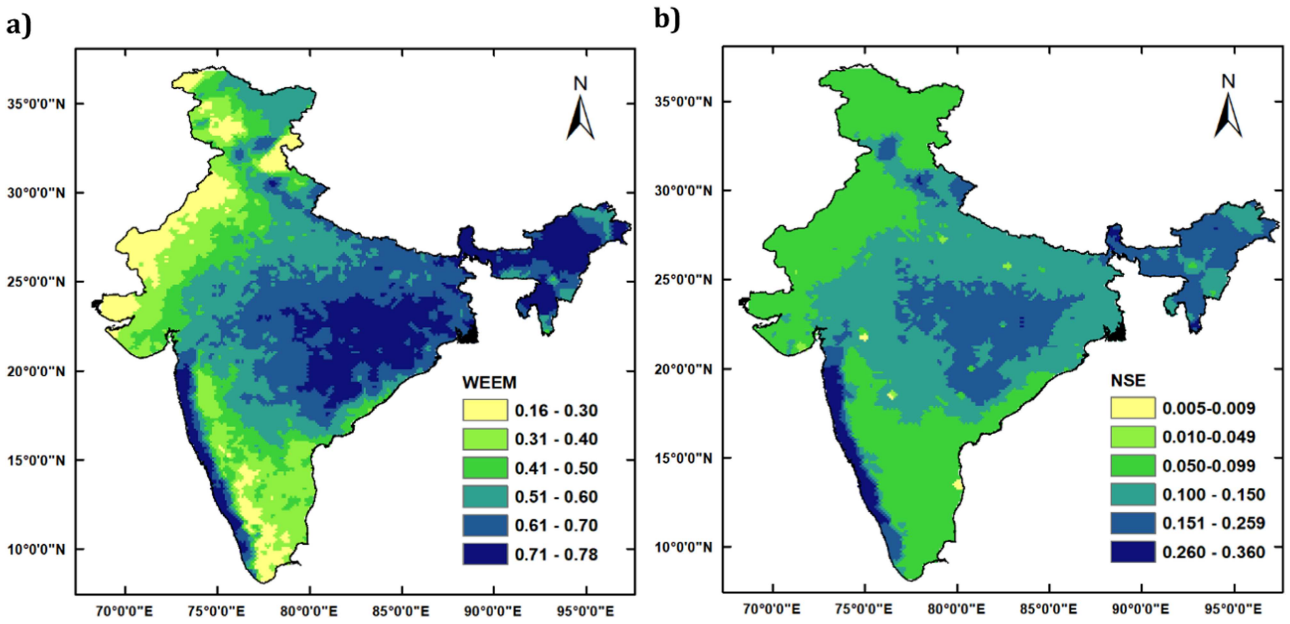

FIG. 7. (a) Spatial distribution of the WEEM estimated using the proposed methodology for all the Indian rainfall time series. WEEM is ranging from a minimum of 0.16 to a maximum of 0.78, and it is classified into six ranges. (b) Spatial distribution of the NSE estimated using the WNN model, and NSE is ranging from a minimum of 0.005 to a maximum of 0.36, and it is classified into six ranges.

scales. For regions with yellow color, the spread of energy distribution is almost nearer to white noise process possessing a low intrinsic predictability when compared to blue spots. The spread of energy to a few scales could be because few external climatic processes govern the rainfall process.

On the contrary, equal spread of energy to all scales signifies strong influence of many external climatic variables making predictability difficult. The corresponding forecasting performance using Eq. (9) shows that the NSE values were ranging from 0– to 0.31 indicating the low intrinsic predictability. The forecasting performance obtained from the WNN reveals a similar kind of distribution as that of intrinsic predictability [see Fig. 7(b)], and similar values of forecasting performance are obtained by other studies such as Refs. 56 and 57 for daily rainfall time series.

As a further step, we also validated the estimated forecasting performance with those obtained from the WNN model. Figure 8 shows the plot between the NSE obtained using Eq. (9) and the actual values got from the best of WNN models for all the time series. The results reveal that the mean square error value is nearer to zero and there is a close correlation between them, indicating the reliability of the proposed WEEM and its linkage with the forecasting performance. Further, this study also shows that the intrinsic predictability of rainfall is varying with space owing to different physical phenomena that are beyond the scope of the present study.

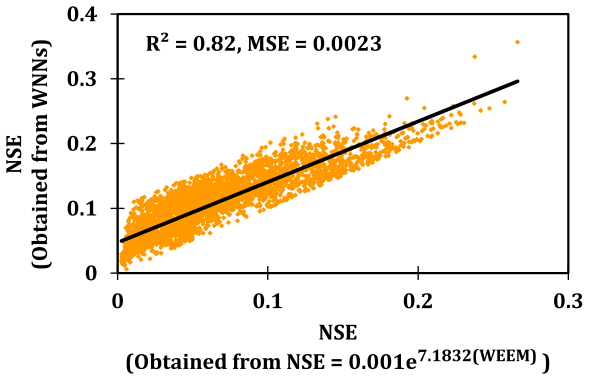

FIG. 8. Scatterplot between actual NSE (ordinate) from the model and the estimated NSE (abscissa) obtained from Eq. (9) for all the Indian rainfall time series. The black line is the best fitted linear equation for the relationship between two scattered values.

V. DISCUSSION

Overall, the above set of cases and analysis showed the efficiency of the WEEM and its linkage between forecasting performances. From the constructed signals with predefined properties, it was observed that the intrinsic predictability is more for $N/S \leq 2$ and gradually decreases for $N/S \geq 2.5$ due to the influence of noise. Investigation of WEEM for the logistic map illustrated the sensitivity of WEEM to changes in the r parameter. The proposed WEEM could capture the nature of the system for different r values, thus showing the applicability of the WEEM to nonlinear time series.

Further, a real-world study shows that the Indian rainfall climatic system has varying intrinsic predictabilities. This finding is in line of agreement with the findings of Refs. 57–59. One of the advantages of the proposed measure is that it considers the dynamics of the process spread across different time scales, which other similarity measures of predictability have not considered explicitly. Furthermore, the proposed measure is linked to forecasting performances. Association of all the available forecasting techniques with WEEM and its linkage with model forecasting performance can lead to improvement in realized predictability.[10,40] Besides, monitoring intrinsic and realized predictability will help in improving the prediction accuracy of the model. To do so, all the existing forecasting techniques must be applied to the same time series and measure the realized predictability in conjunction with intrinsic predictability of time series. The proposed measure can be used for estimating the intrinsic predictability of a time series, understanding the capability of models in capturing the underlying system and among others. In addition to that, the proposed WEEM measure is normalized, handles non-stationarity, and is independent of the length of the data. Therefore, the temporal evolution of the intrinsic predictability can be studied and can provide vital information for change-detection studies.

VI. CONCLUSIONS

In this study, we have proposed a novel measure that combines wavelet analysis and entropy to quantify the intrinsic predictability of a time series. The proposed measure compares the entropy of the wavelet energy distribution of the given time series with the reference white noise process. We have also developed linkage between the proposed measure, WEEM with the popular forecasting performance, and NSE. Using several constructed signals with predefined properties and logistic map model, we have shown that the proposed methodology can capture intrinsic predictability. With the help of the state of the art WNN models, we have also tested the strength of the WEEM–NSE linkage on real-world rainfall time series. The results from the study indicate that the proposed measure can be used as another reliable measure of intrinsic predictability. Thus, WEEM provides an important indicator of the maximum achievable predictability of the time series, which in turn can be applied to specify whether the model is limiting predictability of the system. Therefore, it can help in improving the model. Further studies can be directed toward the application of datasets from diverse areas to strengthen the effectiveness of the proposed approach.

SUPPLEMENTARY MATERIAL

See the supplementary material that comprehends two sections. Section 1 includes a brief description of the construction procedures of constructed signals for three cases, and section 2 includes a detailed description of wavelet neural networks.

ACKNOWLEDGMENTS

M.R. acknowledges the funding received from the SERB, Government of India under Project No. ECR/16/1721. Matjaž Perc was supported by the Slovenian Research Agency (Grant Nos. J4-9302, J1-9112, and P1-0403). A.A. acknowledges the funding support provided by the Indian Institute of Technology Roorkee through Faculty Initiation under Grant No. IITR/SRIC/1808/F.IG.

REFERENCES

[1] E. N. Lorenz, J. Atmos. Sci. **26**, 636 (1969).
[2] M. Duan, "Time series predictability," Doctoral dissertation (Marquette University, 2002).
[3] F. Pennekamp, A. C. Iles, J. Garland, G. Brennan, U. Brose, U. Gaedke, U. Jacob, P. Kratina, B. Matthews, S. Munch, M. Novak, G. M. Palamara, B. C. Rall, B. Rosenbaum, A. Tabi, C. Ward, R. Williams, H. Ye, and O. L. Petchey, Ecol. Monogr. **89**, e01359 (2019).
[4] B. Beckage, L. J. Gross, and S. Kauffman, Ecosphere **2**, 1 (2011).
[5] E. N. Lorenz, in *Predictability of Weather and Climate*, edited by T. Palmer and R. Hagedorn (Cambridge University Press, Cambridge, 1995), pp. 40–58.
[6] R. Wackerbauer, A. Witt, H. Atmanspacher, J. Kurths, and H. Scheingraber, Chaos Soliton. Fract. **4**, 133 (1994).
[7] P. E. Rapp, C. J. Cellucci, K. E. Korslund, T. A. A. Watanabe, and M. A. Jiménez-Montaño, Phys. Rev. E **64**, 016209 (2001).
[8] N. Marwan, N. Wessel, U. Meyerfeldt, A. Schirdewan, and J. Kurths, Phys. Rev. E **66**, 026702 (2002).
[9] C. Bandt and B. Pompe, Phys. Rev. Lett. **88**, 4 (2002).
[10] J. Garland, R. James, and E. Bradley, Phys. Rev. E **90**, 052910 (2014).
[11] C. Song, Z. Qu, N. Blumm, and A.-L. Barabasi, Science **327**, 1018 (2010).
[12] E. Maasoumi and J. Racine, J. Econom. **107**, 291 (2002).
[13] R. Miotto, L. Li, B. A. Kidd, and J. T. Dudley, Sci. Rep. **6**, 26094 (2016).
[14] D. Dahlem, D. Maniloff, and C. Ratti, Sci. Rep. **5**, 11865 (2015).
[15] R. Goody, J. Atmos. Sci. **64**, 2735 (2007).
[16] L. Shuangcheng, Z. Qiaofu, W. Shaohong, and D. Erfu, Int. J. Climatol. **26**, 2131 (2006).
[17] R. Kleeman, J. Atmos. Sci. **59**, 2057 (2002).
[18] D. Cai, R. Kleeman, and A. Majda, Methods Appl. Anal. **9**, 425 (2002).
[19] L. Zhang, H. Li, D. Liu, Q. Fu, M. Li, M. A. Faiz, M. I. Khan, and T. Li, Atmos. Res. **221**, 88 (2019).
[20] Y. Sang, V. P. Singh, J. Wen, and C. Liu, J. Geophys. Res. Atmos. **120**, 5334, https://doi.org/10.1002/2014JD022844 (2015).
[21] J. Doss-Gollin, D. J. Farnham, S. Steinschneider, and U. Lall, Earth Futur. **7**, 734 (2019).
[22] R. Maheswaran and R. Khosa, J. Hydrol. **450–451**, 320 (2012).
[23] A. Barrat, M. Barthelemy, and A. Vespignani, *Dynamical Processes on Complex Networks* (Cambridge University Press, Cambridge, 2008).
[24] J. Kurths, A. Agarwal, R. Shukla, N. Marwan, M. Rathinasamy, L. Caesar, R. Krishnan, and B. Merz, Nonlinear Process. Geophys. **26**, 251 (2019).
[25] M. Rathinasamy, R. Khosa, J. Adamowski, S. Ch, G. Partheepan, J. Anand, and B. Narsimlu, Water Resour. Res. **50**, 9721, https://doi.org/10.1002/2013WR014650 (2014).
[26] N. Ekhtiari, A. Agarwal, N. Marwan, and R. V. Donner, Chaos **29**, 063116 (2019).
[27] Y. F. Sang, D. Wang, J. C. Wu, Q. P. Zhu, and L. Wang, Entropy **13**, 195 (2011).
[28] A. Agarwal, L. Caesar, N. Marwan, R. Maheswaran, B. Merz, and J. Kurths, Sci. Rep. **9**, 1 (2019).
[29] Z. Li and Y.-K. Zhang, Stoch. Environ. Res. Risk Assess. **22**, 507 (2008).
[30] A. Agarwal, N. Marwan, M. Rathinasamy, B. Merz, and J. Kurths, Nonlinear Process. Geophys. **24**, 599 (2017).
[31] R. Maheswaran and R. Khosa, Comput. Geosci. **46**, 284 (2012).
[32] A. Agarwal, R. Maheswaran, J. Kurths, and R. Khosa, Water Resour. Manag. **30**, 4399, (2016).
[33] V. Sehgal, A. Lakhanpal, R. Maheswaran, R. Khosa, and V. Sridhar, J. Hydrol. **556**, 1078 (2018).
[34] D. Liu, Q. Fu, D. Zhao, and T. Li, Hydrol. Sci. J. **62**, 2531 (2017).
[35] P. Xie, Z. Wu, Y. F. Sang, H. Gu, Y. Zhao, and V. P. Singh, J. Hydrol. **560**, 451 (2018).
[36] V. Nourani, K. Roushangar, and G. Andalib, J. Hydrol. **562**, 371 (2018).
[37] C. E. Shannon, Bell Syst. Tech. J. **27**, 379 (1948).
[38] V. P. Singh, Hydrol. Process. **11**, 587 (1997).

[39]P. A. Varotsos, N. V. Sarlis, E. S. Skordas, and M. S. Lazaridou, Phys. Rev. E **70**, 011106 (2004).
[40]P. Xu, L. Yin, Z. Yue, and T. Zhou, Physica A **523**, 345 (2019).
[41]P. S. Addison, *The Illustrated Wavelet Transform Handbook* (CRC Press, 2017).
[42]C. Torrence and G. P. Compo, Bull. Am. Meteorol. Soc. **79**, 61 (1998).
[43]A. K. Alexandridis and A. D. Zapranis, Neural Networks **42**, 1 (2013).
[44]J. Adamowski and K. Sun, J. Hydrol. **390**, 85 (2010).
[45]J. Adamowski and C. Karapataki, J. Hydrol. Eng. **15**, 729 (2010).
[46]I. N. Daliakopoulos, P. Coulibaly, and I. K. Tsanis, J. Hydrol. **309**, 229 (2005).
[47]P. D. Sreekanth, N. Geethanjali, P. D. Sreedevi, S. Ahmed, N. Ravi Kumar, and P. D. Kamala Jayanthi, Curr. Sci. **96**, 933 (2009); available at www.jstor.org/stable/24104683
[48]J. Adamowski, H. Fung Chan, S. O. Prasher, B. Ozga-Zielinski, and A. Sliusarieva, Water Resour. Res. **48**, 1, https://doi.org/10.1029/2010WR009945 (2012).
[49]J. E. Nash and J. V. Sutcliffe, J. Hydrol. **10**, 282 (1970).
[50]T. DelSole, J. Atmos. Sci. **61**, 2425 (2004).
[51]W. Hu and B. C. Si, Hydrol. Earth Syst. Sci. **20**, 3183 (2016).
[52]R. Yan and R. Gao, IEEE Instrum. Meas. Mag. **10**, 40 (2007).
[53]L. L. Trulla, A. Giuliani, J. P. Zbilut, and C. L. Webber, Phys. Lett. A Gen. At. Solid State Phys. **223**, 255 (1996).
[54]D. S. Pai, L. Sridhar, M. R. Badwaik, and M. Rajeevan, Clim. Dyn. **45**, 755 (2014).
[55]M. Rajeevan, J. Bhate, J. D. Kale, and B. Lal, Curr. Sci. **91**, 296 (2006).
[56]C. T. Dhanya and D. Nagesh Kumar, Adv. Water Resour. **33**, 327 (2010).
[57]A. M. Kalteh, Water Resour. Manag. **33**, 3831 (2019).
[58]H. Annamalai, Meteorol. Atmos. Phys. **55**, 61 (1995).
[59]S. Azad, S. Debnath, and M. Rajeevan, Environ. Process. **2**, 717 (2015).
[60]A. Grossmann and J. Morlet, SIAM J. Math. Anal. **15**, 723 (1984).
[61]D. B. Percival and A. T. Walden, *Wavelet Methods for Time SeriesAnalysis* (Cambridge University Press, Cambridge, 2000).
[62]Z. Levnajić and I. Mezić, Chaos **25**, 053105 (2015).
[63]Z. Levnajić and I. Mezić, Chaos **20**, 033114 (2010).
[64]U. Ozturk, N. Marwan, O. Korup, H. Saito, A. Agarwal, M. J. Grossman, M. Zaiki, and J. Kurths, Chaos **28**, 075301 (2018).